

Multiorbital effects on the transport and the superconducting fluctuations in LiFeAs

F. Rullier-Albenque,^{1,*} D. Colson,¹ A. Forget,¹ and H. Alloul²

¹*Service de Physique de l'Etat Condensé, Orme des Merisiers, CEA Saclay (CNRS URA 2464), 91191 Gif sur Yvette cedex, France*

²*Laboratoire de Physique des Solides, UMR CNRS 8502, Université Paris Sud, 91405 Orsay, France*

(Dated: published in Physical Review Letters on November 2, 2012)

Resistivity, Hall effect and transverse magnetoresistance (MR) have been measured in low residual resistivity single crystals of LiFeAs. Comparison with ARPES and Quantum oscillation data implies that four carrier bands unevenly contribute to the transport. However the scattering rates of the carriers all display the T^2 behavior expected for a Fermi liquid. Near T_c low field deviations of the MR with respect to a H^2 variation permit us to extract the superconducting fluctuation (SCF) contribution to the conductivity. Though below T_c the anisotropy of superconductivity is rather small, the SCF display a quasi ideal two-dimensional behavior which persists up to $1.4 T_c$. These results call for a refined theoretical understanding of the multiband behavior of superconductivity in this pnictide.

PACS numbers:

Introduction. The superconductivity (SC) and normal state of the iron-based materials are governed by their electronic structure involving the five iron $3d$ orbitals, as established by band structure calculations and Angle Resolved Photoemission (ARPES) studies [1]. A spin fluctuation exchange mechanism for SC, with a s^\pm symmetry, has been suggested early on, based on the observation of a good nesting between hole and electron Fermi surfaces [2]. This multiband character also highly influences the normal state transport and experimental studies, performed mainly in the BaFe_2As_2 (122) family, show that the electron mobility usually overcomes that of holes [3, 4]. But the conductivity σ and Hall constant R_H do not permit to disentangle the two carrier contributions to the transport.

Unlike other iron-based SC, LiFeAs is a stoichiometric compound with relatively high $T_c \simeq 18$ K without any chemical doping [5, 6], so that it is a nearly compensated semi-metal, rather free from defects. Cleaved single crystals display no surface states [7], and clean ARPES data have evidenced [8, 9] a dominant large hole-like Fermi surface (FS) and a much smaller one centered at the Γ point and two electron-like FS at the corners of the Brillouin zone. The absence of matching between the sizes of the electron and hole FS's being a major difference with other pnictide families, it has been claimed [8] that the poor nesting prevents spin fluctuations driven SC, while an orbital fluctuation mechanism [10] could be more appropriate.

In this letter, we take benefit of the reduced defect content in LiFeAs to take accurate magnetoresistance (MR) data, which together with σ and R_H should permit to determine unambiguously the T dependences of the carrier contents and mobilities. While electron bands are found to dominate the transport as in undoped BaFe_2As_2 , the detailed quantitative comparison with ARPES [8, 9] and de Haas-van-Alphen (dHvA) data [11] shows that the

holes involved in the largest hole band have the weakest mobility in LiFeAs. Furthermore, the MR data permits us a precise determination of the superconducting fluctuations (SCF) contribution to the conductivity using the method we recently established for the cuprates [12, 13]. These SCFs have been so far poorly studied in multiband SC, even in MgB_2 [14], and usually give information on the microscopic properties of the SC state [15]. Here, we find that the SCF paraconductivity can be very well fitted by the gaussian Ginzburg Landau expectation for two dimensional single band SC systems. These results should trigger theoretical studies of SCF taking into account both the multiband aspect and the microscopic origin of SC, such as that initiated in ref. [16].

Resistivity and Hall effect Six samples grown by a self flux technique as detailed in [17] were studied, three with a four-probe configuration (labelled FP 1,2,3) and three with a Van der Pauw configuration [1] (labelled VDP1,2,3). The reproducibility of the data for the in-plane $\rho(T)$ is displayed in Fig.1-a, the small differences (20% at most at room T) being ascribed to errors in the sample geometrical factors. The SC transition curves in the inset of Fig.1-a evidence increasing T_c values (15.5 K to 18.2 K) for decreasing $\rho(T_c)$, except for FP1. As shown below, the data can be fitted with $\rho(T) = \rho_0 + AT^2$ below $\simeq 30$ K. For our best samples FP1 and FP2, $\rho_0 \sim 1.3\mu\Omega.cm$ corresponds to residual resistivity ratios $RRR = \rho(300K)/\rho_0 \simeq 250$, five times larger than previously reported [2, 3, 19, 20]. Comparing all those data [17], we find that both ρ_0 and A increase with decreasing T_c , *i.e* Matthiessen's rule does not apply and $\rho(T)$ cannot be analysed in a *single-band model in LiFeAs*.

Whatever the temperature, we found that the Hall voltage is linear in field up to 14T. The similar negative Hall coefficients R_H , reported in Fig.1-b for three samples with slightly different T_c , show that electrons dominate

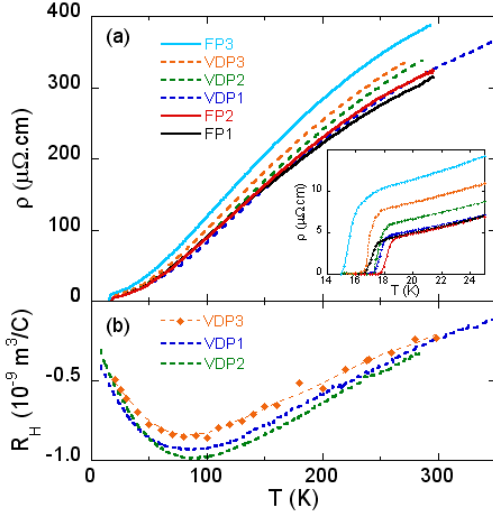


FIG. 1: (color on line) (a) In plane-resistivity versus temperature for the six samples of LiFeAs measured. An expanded view of the superconducting transitions is reported in the inset. Except for one sample, one can see a correlation between the values of T_c and those of the residual resistivity. (b) Hall coefficient versus temperature for the three samples mounted in the Van der Pauw configuration.

the transport in this nearly compensated compound as in the nonmagnetic state of BaFe_2As_2 [3]. The broad minimum of $R_H(T)$, seen around 100K, coincides with the observed change of curvature in the $\rho(T)$ curves. $R_H(T)$ tends towards zero with increasing T , which signals that the mobilities of holes and electrons become similar. This behaviour bears some resemblance with that found in overdoped Co-doped BaFe_2As_2 samples which also exhibit a minimum around 100K, albeit less pronounced, and a similar increase towards room T [3].

Transverse magnetoresistance. The small values of the residual resistivity ρ_0 permitted us to perform accurate measurements of the transverse MR above T_c up to 160K. As shown in Fig.2a, for $T \gtrsim 45\text{K}$, the MR increases as H^2 in the whole field range investigated here ($H \leq 14\text{T}$). At lower T (see Fig.2b), the low H increase of conductivity detected when approaching T_c is reminiscent of the contribution of superconducting fluctuations as evidenced in YBCO [13]. These SCFs will be analysed later, but we shall focus first on the normal state which is fully restored beyond a threshold field $H'_c(T)$, allowing us to define the MR coefficient $a(T)$ as

$$\delta\rho/\rho(T, 0) = [\rho(T, H) - \rho(T, 0)]/\rho(T, 0) = a(T)H^2 \quad (1)$$

As shown in the inset of Fig.2a, $a(T)$ is found identical in FP1 and FP2 and to decrease by about three orders of magnitude from T_c to 160K.

Compensated two-band model The most natural approach to analyse these transport properties is within a two-band model. The transport coefficients are related

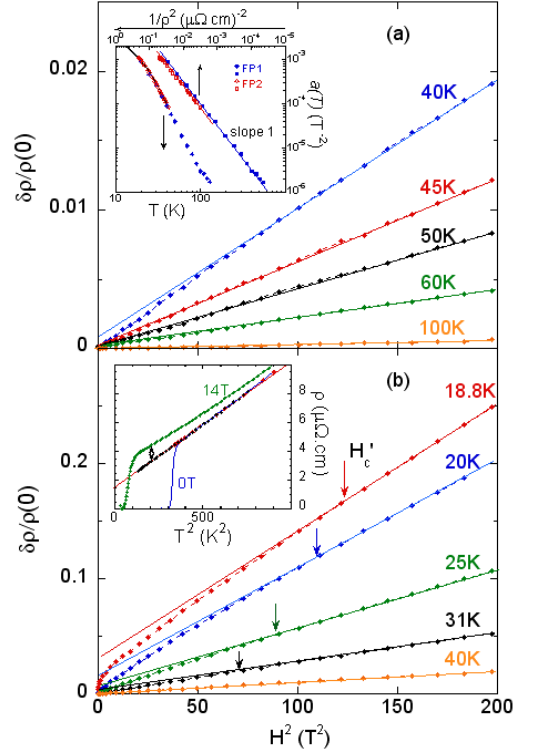


FIG. 2: (color on line) The transverse magnetoresistance measured in FP1 is plotted as a function of H^2 for $T > 40\text{K}$ in (a) and below 40K in (b). At high T , the MR is linear in H^2 whatever H while it recovers this variation only above a given threshold field H'_c (indicated by arrows) for $T \lesssim 50\text{K}$. In the inset of (a), the MR coefficient $a(T)$ of Eq.1 is plotted versus T and $1/\rho^2$ for FP1 and FP2. The full lines of slope 1 indicate that Kohler's rule is very well obeyed (see text). In the inset of (b) the resistivity measured in 14 T field down to 10K is plotted versus T^2 for FP1, together with the extrapolated zero field data.

to the respective conductivities σ_h , σ_e and mobilities μ_h , μ_e of the holes and electrons by:

$$\rho^{-1} = \sigma = \sigma_e + \sigma_h \quad (2)$$

$$R_H = (\sigma_h\mu_h - \sigma_e\mu_e)/\sigma^2 \quad (3)$$

$$\delta\rho/\rho(T, 0) = \sigma_e\sigma_h(\mu_h + \mu_e)^2 H^2/\sigma^2 \quad (4)$$

In undoped pnictides such as LiFeAs one expects equal number of electrons and holes $n_e = n_h = n$ [8, 9] and the two last equations condense into $\sigma R_H = \mu_h - \mu_e$ and $a(T) = \mu_e\mu_h$, so that the data permit us to deduce the T variations of μ_h , μ_e and n . In particular, with $R = 1/n_e$, these equations can be combined into

$$a(T) = (R^2 - R_H^2)/4\rho^2(T, 0). \quad (5)$$

We can see in fig.2-a that $a(T)$ scales as ρ^{-2} , that is Kohler's rule [23] is well obeyed in LiFeAs, which indicates that $R^2 - R_H^2$ has a weak T dependence. We show

in Fig.3c that both scattering rates display a T^2 variation up to $\sim 70\text{K}$ [17], with $\mu_e/\mu_h \sim 1.5$ (see Fig.3b) [24], and that the number of carriers is nearly T independent below 120K. At higher T , thermal population of narrow bands might induce an increase of $n(T)$ [2], in analogy with the proposal we have done to explain the transport properties of $\text{Ba}(\text{Fe}_{1-x}\text{Co}_x)_2\text{As}_2$ [3].

Comparison with ARPES and dHvA: beyond the two-band model However, the deduced carrier content $n \sim 0.09$ el/Fe being twice smaller than that given by ARPES or by dHvA [9, 11], this implies that the two-band model only allows us to determine separate average parameters for the holes and electrons. Indeed, we do know from ARPES data [8, 9] that hole carriers are located in a small inner (ih) band included in a large outer (oh) band. Similarly, it has been suggested [25] that, due to strong spin-orbit coupling, the electron bands should not be considered as two crossed degenerate elliptic pockets. As found in dHvA experiments in both LiFeP and LiFeAs [11], they split into an inner (ie) band included in an outer one (oe). The carrier mobilities are expected to differ substantially for these four bands, and the MR coefficient has now a more complicated expression than given in eq.4 [26]:

$$H^{-2}\Delta\rho/\rho(T, 0) = \sigma_e\sigma_h(\mu_e + \mu_h)^2/\sigma^2 + \sigma_h A_h/\sigma + \sigma_e A_e/\sigma \quad (6)$$

with $A_h = \sigma_{ih}\sigma_{oh}(\mu_{ih} - \mu_{oh})^2/\sigma_h^2$, where μ_h is now an effective hole band mobility given by $\sigma_h\mu_h = \sigma_{ih}\mu_{ih} + \sigma_{oh}\mu_{oh}$ and an effective number of holes is defined by $\sigma_h = n_h^{eff}e\mu_h$. Similar expressions hold for the electron bands.

To approach a solution we may use for the T independent carrier contents those obtained from ARPES and dHvA experiments $n_{oh} \sim 0.16$ h/Fe , $n_{ih} \sim 0.03$ h/Fe , $n_{oe} \sim 0.11$ el/Fe and $n_{ie} \sim 0.08$ el/Fe for the outer and inner hole (electron) bands respectively. As we are still lacking sufficient experimental information, a unique solution cannot be acquired. However dHvA results imply that the mobilities for the two electron bands are comparable. Matching the data with all these assumptions yields a strong differentiation of the two hole bands with a surprisingly much lower mobility for the outer band compared to the inner one. Also, imposing $\mu_{oe} \simeq \mu_{ie}$ puts some constraints on the value of n_h^{eff} that cannot be larger than ~ 0.06 h/Fe [17]. A solution with $n_h^{eff} = 0.05$ h/Fe whatever T is illustrated in Fig.3c and gives a ratio between the electron (hole) mobilities respectively of $\mu_{ie}/\mu_{oe} = 3 - 6$ and $\mu_{ih}/\mu_{oh} \sim 17$. It corresponds to $n_e^{eff} \sim 0.13$ el/Fe and it results in similar values of the effective electron and hole mobilities [17], which would justify why Kohler's rule is obeyed in this compound. Whatever the value taken for n_h^{eff} in the range considered, we always find that the scattering rates for the different carriers increase as T^2 up to $\sim 70\text{K}$, as seen in Fig.3c. This confirms a Fermi liquid behavior for both

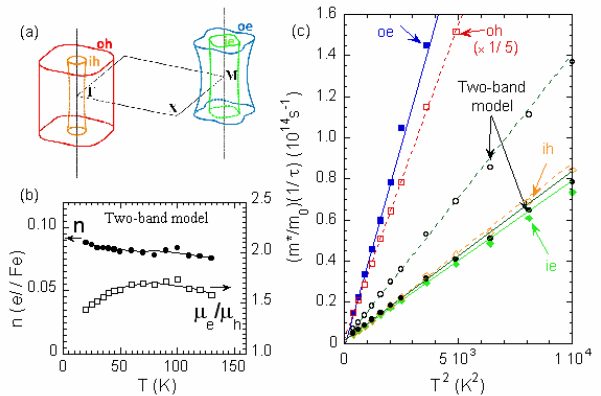


FIG. 3: (color on line) **a**: schematic view of the Fermi surfaces sheets of LiFeAs. **b**: number of carriers and mobility ratio extracted from the compensated two-band model. **c**: Scattering rates deduced in a two-band analysis (circles) and for the four band solution given in the text, plotted versus T^2 . Full (empty) symbols and full (dashed) linear fits are for the electrons (holes). Notice that the data for the oh band has been divided by 5.

holes and electrons in agreement with density functional theory and dynamical mean Field (DFT+DMFT) calculations [25].

The $T = 0$ extrapolated values correspond to mobilities ~ 1000 cm^2/Vs for the smallest hole and electron bands, that is, using a Fermi velocity $v_F \sim 1 \cdot 10^5$ m/s [27] and an effective mass $m^* \simeq 4m_0$ [11], to mean free paths ≈ 2000 \AA , in agreement with the high purity of our FP1 sample. Much faster relaxation is observed for the outer hole band which is exclusively constructed from the d_{xy} orbital, for which a stronger incidence of correlations on m^* and the scattering rates is expected from DFT+DMFT calculations [25, 28].

Superconducting fluctuation contribution to conductivity. We detail in [17] why the low field deviations from a H^2 behavior of the MR cannot be associated with a saturation of the normal state MR. This is confirmed experimentally, as such deviations were not detected in LiFeP, which has a lower $T_c = 7\text{K}$ than LiFeAs, with a similar band structure and residual resistivity as our samples [3]. Following our extensive study done in cuprates [13], the SCF contribution to the conductivity is given by $\Delta\sigma_{SF}(T) = \rho^{-1}(T) - \rho_n^{-1}(T)$, where $\rho_n(T)$ is the $H = 0$ extrapolation of the H^2 variation of the normal state MR. Let us notice here that $\Delta\sigma_{SF}(T)$, which does not exceed 3% of the normal state values (see fig.2b), would be extremely difficult to extract directly from the $\rho(T)$ curves.

For our samples with the highest T_{c0} , the $\Delta\sigma_{SF}$ data reported in a log-log scale in Fig.4 as a function of the reduced temperature $\epsilon = \ln(T_c/T_{c0})$ resemble those found in cuprates [13]. After an initial power law behavior, $\Delta\sigma_{SF}(T)$ displays a cut-off, and only becomes negligible

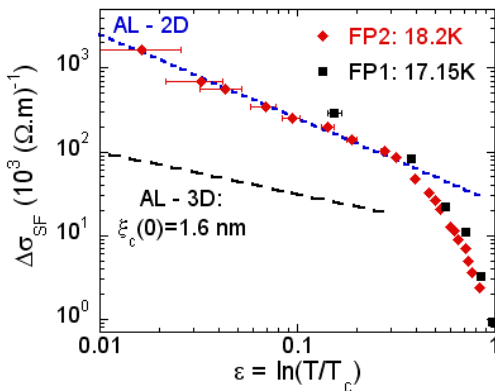


FIG. 4: (color on line) Superconducting fluctuation conductivity $\Delta\sigma_{SF}$ for samples FP1 and FP2 as a function of $\epsilon = \ln(T/T_{c0})$, where T_{c0} is taken at the midpoint of the transition. The error bars for ϵ were determined using T_c values at 25% and 75% of the resistive transition. Estimates of the AL contribution in dimensions 2 and 3 are displayed as dashed lines for comparison.

for $\epsilon \sim 1$. This larger SCF regime $\sim 2.5 T_c$ than that we did find in cuprates points towards a 2D character. This is better seen from the good fit with the 2D Aslamazov-Larkin formula

$$\Delta\sigma^{AL}(T) = (e^2/16\hbar s) \epsilon^{-1}, \quad (7)$$

for $0.017 \lesssim \epsilon \lesssim 0.3$, corresponding to $T = 1.02$ to $1.4T_c$, without any fitting parameter except the interlayer distance s taken here as the lattice parameter value $c = 6.36\text{\AA}$. The value of T_c is taken here at the midpoint of the transition but our conclusion remains valid for slightly different T_c determinations as shown by the error bars for ϵ in Fig.4.

These 2D SCFs appear at first sight difficult to reconcile with the 3D character of the normal and SC states in LiFeAs suggested by the weak anisotropies of resistivity and upper-critical field H_{c2} [20, 29, 30] (see also [17]). Using for instance a single-band scheme to deduce the coherence length along the c -axis from H_{c2} , we find $\xi_c \sim 16\text{\AA}$, that is more than twice the interlayer spacing. So one would expect for 3D fluctuations the much smaller contribution to the conductivity shown in Fig.4. All this suggests that the present result is specific to multiband effects and that, above T_c , the fluctuating pairs are driven by a single 2D band. In view of our discussion above on the normal state, only the outer hole pocket that originates from in-plane d_{xy} orbitals is purely 2D [25, 28, 31].

It is worth comparing our results in LiFeAs with the case of MgB_2 , a presumably much simpler multiband SC which also displays a rather low H_{c2} anisotropy factor ~ 2 at T_c . It has been proposed [14] that the SCFs are governed by a unique critical mode, which is dominated for $T \gg T_c$ by the quasi 2D σ bands with the larger

SC gap. However, near T_c , the critical mode should recover a 3D character due to both band contributions and the paraconductivity should diverge slightly slower than $\sim 1/\sqrt{\epsilon}$. Preliminary data [32] have been analysed as suggesting 2D SCFs but, to our knowledge, no more reliable experimental work has been performed since.

Concerning the properties of the SC gaps in LiFeAs, they are found weakly anisotropic by ARPES, the largest $\Delta = 5 - 6\text{meV}$ for the small 3D hole pocket, while $\Delta = 3 - 4\text{meV}$ for the other bands [9, 31], including the large 2D hole band. In that context one should rather expect a pronounced 3D character for the SCFs in LiFeAs [33].

Discussion. In the specific case of pnictides, it has been underlined recently [16] that the SCFs are indeed expected to behave differently as, contrary to the case of MgB_2 [14], the pairing should be dominated by interband spin fluctuation interactions [34]. These authors have shown that, in such a case, the critical mode controlling the SCFs should have a simpler relation to the various bands, so that the AL formula known for single band SC should remain valid either in 2D or 3D. Further experimental investigations of the SCFs along the same lines in other pnictide families would be necessary to get a more complete understanding of SCFs in these multiband compounds. For instance, one needs to ascertain whether the SCFs are dominated by a 3D contribution in the hole doped $\text{BaKFe}_2\text{As}_2$, as has been suggested from an investigation of the diamagnetism above T_c [35].

To conclude, we emphasized here the relevance of MR data to unveil new physical phenomena. Our data give indications which should help to investigate the incidence of spin fluctuations on the carrier scattering in the normal state and on the SC pairing in this specific LiFeAs system. On the other hand, it would be interesting to study whether other proposals such as orbital fluctuations or p-wave SC [10, 36] might provide a natural explanation for these 2D SCFs. Unveiling the origin of these 2D SCFs should therefore give useful hints to clarify the mechanism of SC in LiFeAs.

This work has been performed within the "Triangle de la Physique" and was supported by ANR grant "PNICTIDES". We thank L. Benfatto, R. Valenti and A. Coldea for helpful scientific exchanges about the interesting specifics of this LiFeAs compound.

* Electronic address: florence.albenque-rullier@cea.fr

- [1] For a review, see D.C. Johnston, Adv. Phys. **59**, 803 (2010).
- [2] I.I. Mazin and J. Schmalian, Physica C (Amsterdam) **469**, 614 (2009).
- [3] F. Rullier-Albenque, D. Colson, A. Forget, and H. Alloul, Phys. Rev. Lett **103**, 057001 (2009).
- [4] S. Kasahara, T. Shibauchi, K. Hashimoto, K. Ikada, S. Tonegawa, R. Okazaki, H. Shishido, H. Ikeda, H. Takeya,

- K. Hirata, T. Terashima, and Y. Matsuda, *Phys. Rev. B* **81**, 184519 (2010).
- [5] J.H. Tapp, Z. Tang, B. Lv, K. Sasmal, B. Lorenz, P.C.W. Chu, and A.M. Guloy, *Phys. Rev. B* **78**, 060505 (2008).
- [6] M.J. Pitcher, D.R. Parker, P. Adamson, S.J.C. Herkelrath, A.T. Boothroyd, and S.J. Clarke, *Chem. Commun.* **41**, 5918 (2008).
- [7] A. Lankau, K. Koepf, S. Borisenko, V. Zabolotnyy, B. Büchner, J. van den Brink, and H. Eschrig, *Phys. Rev. B* **82**, 184518 (2010).
- [8] S.V. Borisenko, V.B. Zabolotnyy, D.V. Evtushinsky, T.K. Kim, I.V. Morozov, A.N. Yaresko, A.A. Kordyuk, G. Behr, A. Vasilief, R. Follath, and B. Büchner, *Phys. Rev. Lett.* **105**, 067002 (2010).
- [9] K. Umezawa, Y. Li, H. Miao, K. Nakayama, Z-H Liu, P. Richard, T. Sato, J.B. He, D-M Wang, G.F. Chen, H. Ding, T. Takahashi, and S-C Wang, *Phys. Rev. Lett.* **108**, 037002 (2012).
- [10] H. Kontani and S. Onari, *Phys. Rev. Lett.* **104**, 157001 (2010).
- [11] C. Putzke, A.I. Coldea, I. Guillamon, D. Vignolles, A. McCollam, D. LeBoeuf, M.D. Watson, I.I. Mazin, S. Kasahara, T. Terashima, T. Shibauchi, Y. Matsuda, and A. Carrington, *Phys. Rev. Lett.* **108**, 047002 (2012).
- [12] F. Rullier-Albenque, H. Alloul, C. Proust, D. Colson, and A. Forget, *Phys. Rev. Lett.* **99**, 027003 (2007).
- [13] F. Rullier-Albenque, H. Alloul and G. Rikken, *Phys. Rev. B* **84**, 014522 (2011).
- [14] A.E. Koshelev, A.A. Varlamov and V.M. Vinokur, *Phys. Rev. B* **72**, 064523 (2005).
- [15] A. Larkin and A.A. Varlamov, *Theory of fluctuations in superconductors*, (Oxford University Press), Oxford, 2005.
- [16] L. Fanfarillo, L. Benfatto, S. Caprara, C. Castellani, and M. Grilli, *Phys. Rev. B* **79**, 172508 (2009).
- [17] See supplementary material for experimental details and more explanations.
- [18] L.J. van der Pauw, *Philips Res. Repts* **13**, 1-9 (1958).
- [19] B. Lee, S. Khim, J.S. Kim, G.R. Stewart, and K.H. Kim, *Europhys. Lett.* **91**, 67002 (2010).
- [20] Y.J. Song, J.S. Ghim, B.H. Min, Y.S. Kwon, M.H. Jung, and J-S. Rhyee, *Appl. Phys. Lett.* **96**, 212508 (2010).
- [21] O. Heyer, T. Lorenz, V.B. Zabolotnyy, D.V. Evtushinsky, S.V. Borisenko, I. Morozov, L. Harnagea, S. Wurmehl, C. Hess, and B. Büchner, *Phys. Rev. B* **84**, 064512 (2011).
- [22] S. Kasahara, K. Hashimoto, H. Ikeda, T. Terashima, Y. Matsuda, and T. Shibauchi, *Phys. Rev. B* **85**, 060503 (2012).
- [23] A.B. Pippard, *Magnetoresistance in Metals* (Cambridge Univ. Press) 1989.
- [24] The values of the electron and hole mobilities, and their ratio, determined here are very different from those reported in ref.[3] in which $\mu_e/\mu_h \sim 10$. This comes from numerical errors in their determination of mobilities from their experimental data. The correct estimate $\mu_e/\mu_h \sim 1.4$ is very similar to ours.
- [25] J. Ferber, K. Foyevtsova, R. Valenti and H.O. Jeschke, *Phys. Rev. B* **85**, 094505 (2012).
- [26] H-H. Kuo, J6H. Chu, S.C. Riggs, L. Yu, P.L. McMahon, K. De Greve, Y. Yamamoto, J.G. Analytis, and I.R. Fisher, *Phys. Rev. B* **84**, 054540 (2011).
- [27] A.A. Kordyuk, V.B. Zabolotnyy, D.V. Evtushinsky, T.K. Kim, L.V. Morozov, M.L. Kulić, R. Follath, G. Behr, B. Büchner, S. V. Borisenko, *Phys. Rev. B* **83**, 134513 (2011).
- [28] Z. P. Yin, K. Haule, and G. Kotliar, *Nature Materials* **10**, 932-935 (2011).
- [29] N. Kurita et al., *J. Phys. Soc. Jpn.* **80**, 013706 (2011).
- [30] K. Cho, H. Kim, M.A. Tanatar, Y.J. Song, Y.S. Kwon, W.A. Coniglio, C.C. Agosta, A. Gurewich, and R. Prozorov, *Phys. Rev. B* **83**, 060502 (2011).
- [31] S. V. Borisenko *et al.*, *Symmetry* **4**, 251 (2012).
- [32] A.S. Sidorenko *et al.*, *J. Supercond. Nov. Magn.* **17**, 211 (2004).
- [33] L. Benfatto, private communication.
- [34] N. Qureshi, P. Steffens, Y. Drees, A.C. Komarek, D. Lamago, Y. Sidis, L. Harnagea, H-J. Grafe, S. Wurmehl, B. Büchner, and M. Braden, *Phys. Rev. Lett.* **108**, 117001 (2012).
- [35] J. Mosqueira, J.D. Dancausa, F. Vidal, S. Salem-Sugui, Jr, A.D. Alvarenga, H-Q. Luo, Z-S. Wang, and H-H. Wen, *Phys. Rev. B* **83**, 094519 (2011).
- [36] T. Hänke, S. Sykora, R. Schlegel, D. Baumann, L. Harnagea, S. Wurmehl, M. Daghofer, B. Büchner, J. van den Brink, and C. Hess, *Phys. Rev. Lett* **108**, 127001 (2012).

SUPPLEMENTARY MATERIAL

Samples and transport measurements Single crystals of LiFeAs were grown using a self-flux method. Lumps of Li and powders of FeAs and As in the molar ratio 3:2:3 were placed in an alumina crucible in an argon glove box. The crucible was inserted into a ceramic container covered by a cap and sealed in an evacuated quartz tube. The samples were heated to 1090°C with a rate of 175°C/h, held at this temperature for 4h then cooled down to 800°C at 6°C/h and then more rapidly to room temperature. Clean crystals of typical dimensions 5x5x0.05mm³ were mechanically extracted from the flux. A Fe:As ratio of 1:1 has been confirmed by electron microprobe.

Six different samples from the same batch with different geometries were studied. They were cleaved from larger crystals to thicknesses ranging from 18 to 60μm. Electrical contacts were made using silver epoxy. Owing to the very fast degradation of the surfaces under air exposure, the samples were covered with Apiezon N-grease immediately after putting the contacts and very rapidly inserted in the cryostat.

Hall effect measurements were performed in the Van der Pauw configuration [1] for three samples labelled VDP1,2,3 while standard 4-probe technique was used for magnetoresistance measurements in three other samples (labelled FP1,2,3). The Hall effect was measured by exchanging the voltage and current probes in the diagonal directions of the VdP samples either in a fixed 14T magnetic field (VDP1 and 2) or by sweeping the magnetic field up to 14T (VDP3). In all cases, it was checked that the Hall voltage increases linearly with magnetic field, allowing us to determine unambiguously the Hall coefficient. The transverse magnetoresistance (MR) has been measured on the samples FP1 and 2 at fixed temperature by sweeping the magnetic field from -14 to 14T and taking the symmetric part of the signal in order to eliminate any spurious component due to misalignment of the contacts. As the MR becomes rather small above $T > 100\text{K}$ (usually less than 0.05% at 14T) great care has been taken to ensure that the temperature remains constant during the magnetic field ramp. We have used a cernox sensor which has been calibrated in magnetic field and the temperature was then regulated by compensating the incidence of the field on the sensor value.

Characteristics of the different samples The transport and superconducting parameters found for the different samples studied here are gathered in Table I and compared to some data published in the literature. Diamagnetic shielding was also measured for sample VDP1 and gave an onset T_c value of 17.4K with a transition width of 2K, in close agreement with the transport measurements. One can see that the coefficient A is strongly dependent on the purity of the sample. This

TABLE I: The transport parameters for the different samples studied are compared with those reported in ref.[2, 3]. The values of T_c are taken at the mid-point of the resistive transition. The residual resistivities ρ_0 have been determined by fitting the zero field $\rho(T)$ curves with a T^2 dependence $\rho(T) = \rho_0 + AT^2$. The residual resistivity ratio RRR is given by $\rho(300\text{K})/\rho_0$.

Sample	T_c (K)	ρ_0 ($\mu\Omega.cm$)	RRR	A ($n\Omega.cm/K^2$)
VDP1	17.75	4.15	80	9.7
VDP2	17.6	2.93	119	9.3
VDP3	17	4.55	79	9.5
FP1	18.2	1.47	225	8.8
FP2	17.15	1.21	263	9.3
FP3	15.6	6.34	62	12.7
Ref.[2]	17.75	15.2	38	22
Ref.[3]	17.3	13	53	20

means that, as could be expected for a multiband compound, Matthiessen's rule is not obeyed. Consequently, the comparison between the values of A and the electronic specific heat coefficient through the Kadowaki-Woods ratio, which is used to estimate the strength of electronic correlations in single-band metals, cannot be done so straightforwardly here.

Resolution of the problem beyond the two-band model As explained in the text, we have to solve a problem with four unknown mobilities and only three experimental parameters. From dHvA results we know that the mobilities for the two electron bands are similar and must be larger than those of the hole bands. If we consider the limit where they are equal, that is $\mu_{ie} = \mu_{oe}$ with $n_e^{eff} = n_{ie} + n_{oe}$, we find that the mobility of the inner hole band is much larger than that of the outer one, and also larger than the electron mobility. In that case, the effective number of holes defined as $\sigma_h = n_h^{eff} \mu_h$ is equal to n_{ie} taken equal here to $0.03h/Fe$.

A more physical solution can thus be obtained by increasing n_h^{eff} , which consequently lets the hole outer band participate to the transport and slightly differentiates the two electron bands, with $\mu_{oe} \lesssim \mu_{ie}$. However if n_h^{eff} is taken too large, typically $\gtrsim 0.06h/Fe$, the mobilities for the two electron bands become very different, in contradiction with the dHvA results. Consequently $0.03 < n_h^{eff} < 0.06$ is required to match the transport data together with the ARPES and dHvA results. The solution given in the text is obtained for $n_h^{eff} = 0.05h/Fe$. At this stage we are not able to better refine the resolution of the problem and n_h^{eff} is taken T independent, which means that the ratio between the mobilities of the two hole bands is assumed to remain constant with temperature. Though this is not justified, this hypothesis should not distort the main conclusions drawn from this analysis.

Technically, the resolution of the problem then con-

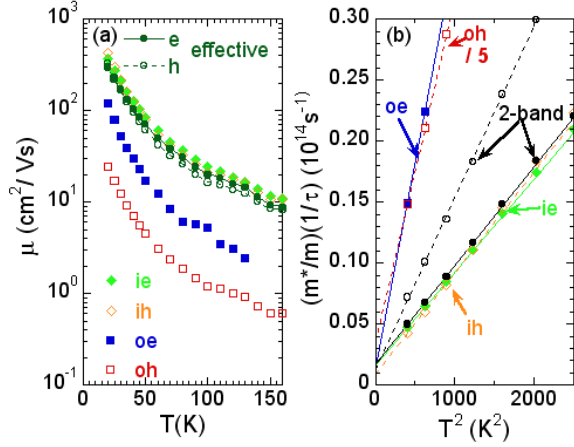


FIG. 5: (color on line) (a): electron and hole mobilities for the four different bands by using a realistic model differentiating the four bands as explained in the text. The effective mobilities for the electron and hole bands are also plotted and found nearly identical to the larger mobilities of the inner bands. (b) Scattering rates weighted by their effective masses plotted versus T^2 for the electrons and holes, using either a compensated two band model or the four band analysis considered in a. Lines are linear fitting curves.

sists in extracting the different mobilities of the electrons and the effective mobility of the holes from Eqs. 2, 3 and 6 of the text. The values of the number of holes in the two different bands ($n_{ih} = 0.03$, $n_{oh} = 0.16$) and $n_h^{eff} = 0.05$ imply $\mu_{oh} \ll \mu_{ih}$ and the term A_h in Eq.6 can be neglected. The second term $\sigma_e A_e / \sigma$ represents at most $\sim 25\%$ of the total MR coefficient. Only one solution is found at each temperature, giving the different mobilities plotted in fig.5a. One can see that the effective mobilities found for the holes and electrons are nearly equal. This explains why Kohler's rule is well obeyed in this compound. Indeed in a two-band model, this rule directly follows from the fact that the two different types of carriers have the same mobility.

The low temperature behavior of the corresponding scattering rates weighted by the effective mass is displayed in Fig.5-b where good fits with a T^2 law is found up to ~ 70 K. Although the actual $T = 0$ extrapolated values has to be considered with caution as they depend on the chosen value of n_h^{eff} , we have checked that we always find comparable values of the order of $2 \cdot 10^{12} \text{s}^{-1}$ for all the carriers except for the outer hole band. This would yield mean free paths for the electrons about 5 times larger than those found in dHvA experiments [4] and thus let us foresee that the inner hole band should be also observed by dHvA in our cleanest samples.

Possible deviations of the MR from a H^2 behavior
The expressions (Eqs. 3 and 4) given in the text for

the Hall coefficient and the transverse MR are the first order approximation in H^2 . At a higher order, we get:

$$\rho_{xy}(H) = \frac{(\mu_h \sigma_h - \mu_e \sigma_e) H}{(\sigma_h + \sigma_e)^2 + (\sigma_e \mu_h - \sigma_h \mu_e)^2 H^2} \quad (8)$$

$$\frac{\delta \rho}{\rho(0)} = \frac{\sigma_e \sigma_h (\mu_e + \mu_h)^2 H^2}{(\sigma_h + \sigma_e)^2 + (\sigma_e \mu_h - \sigma_h \mu_e)^2 H^2} \quad (9)$$

This can introduce some saturation of the Hall coefficient and MR when the second term in the denominator $(\sigma_e \mu_h - \sigma_h \mu_e)^2 H^2$ becomes comparable or larger than σ^2 . For a compensated material with $n_e = n_h$ this term is always zero and no saturation of the Hall resistivity nor magnetoresistance is expected with increasing magnetic field. Deviations from a H^2 behavior can in principle occur if $n_e \neq n_h$. However, this is unlikely here as we found that the Hall effect that should display the same effect remains linear in H within a $5 \cdot 10^{-3}$ accuracy in the same temperature range. Moreover, using the values of the effective mobilities found above, we expect at most a change of slope of $\sim 4\%$ for the MR at 20K between 0 and 14T, while the observed deviation corresponds to nearly a factor 2. Consequently the downward shifts observed at low magnetic field can only arise from the contribution of superconducting fluctuations and its suppression by the magnetic field.

Determination of the upper-critical fields Fig.6 shows the resistive superconducting transitions of the sample FP2 for different magnetic fields up to 14T parallel (a) or perpendicular (b) to the c-axis. Only a small broadening of the SC transitions is observed with increasing H , allowing us to define the critical temperature $T_c(H)$ at the mid-point of the resistive transition for each magnetic field quite precisely. For both orientations of the magnetic field, the increase of H_{c2} with decreasing T shows a linear dependence as shown by the full lines in Fig.6c with a ratio between the slopes of ~ 2.2 in excellent agreement to what was found in earlier reports [2, 3].

* Electronic address: florence.albenque-rullier@cea.fr

- [1] L.J. van der Pauw, Philips Res. Repts **13**, 1-9 (1958).
- [2] O. Heyer, T. Lorenz, V.B. Zabolotnyy, D.V. Evtushinsky, S.V. Borisenko, I. Morozov, L. Harnagea, S. Wurmehl, C. Hess, and B. Büchner, Phys. Rev. B **84**, 064512 (2011).
- [3] S. Kasahara, K. Hashimoto, H. Ikeda, T. Terashima, Y. Matsuda, and T. Shibauchi, Phys. Rev. B **85**, 060503 (2012).
- [4] A. Coldea, private communication.

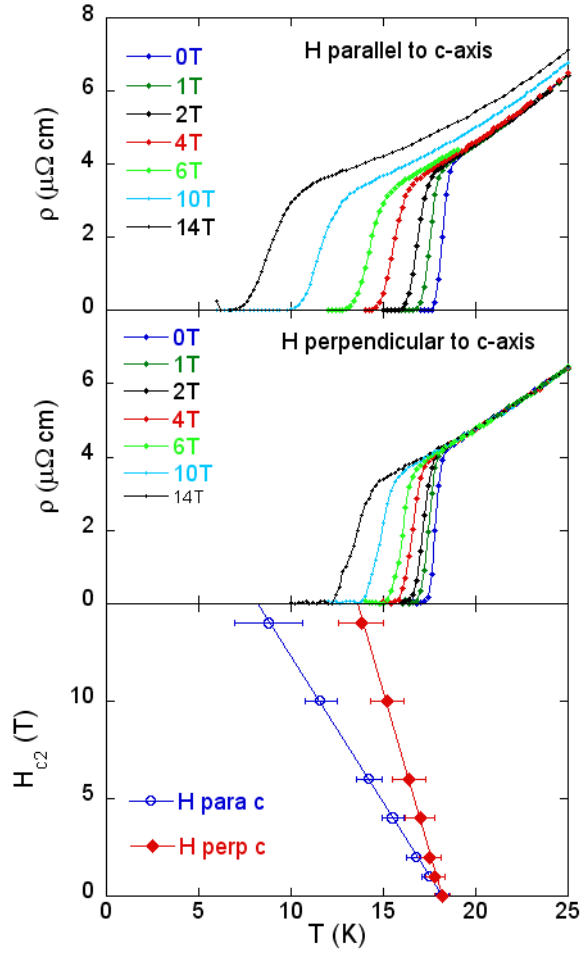


FIG. 6: (color on line) Resistive transitions of the sample FP2 at different magnetic fields applied parallel (a) and perpendicular (b) to the c-axis. (c) Upper-critical fields $H_{c2}(T)$ for the magnetic field applied parallel (empty circles) and perpendicular (full diamonds) to the c-axis. The error bars represent the transition widths measured at 10-90% of the resistive transitions.